

See discussions, stats, and author profiles for this publication at: <https://www.researchgate.net/publication/231629701>

# Host–Guest Interactions in P1, SUZ-4, and ZSM-57 Zeolites Containing N,N,N,N',N',N'-Hexaethylpentanediammonium Ion as a Guest Molecule

ARTICLE in THE JOURNAL OF PHYSICAL CHEMISTRY B · SEPTEMBER 2001

Impact Factor: 3.3 · DOI: 10.1021/jp0101413

---

CITATIONS

27

---

READS

15

5 AUTHORS, INCLUDING:



Byoung Joon Ahn

Chonbuk National University

40 PUBLICATIONS 189 CITATIONS

SEE PROFILE

# Host–Guest Interactions in P1, SUZ-4, and ZSM-57 Zeolites Containing *N,N,N,N',N',N'*-Hexaethylpentanediammonium Ion as a Guest Molecule

Woon Chang Paik,<sup>†</sup> Chae-Ho Shin,<sup>‡</sup> Jong Myung Lee,<sup>§</sup> Byoung Joon Ahn,<sup>§</sup> and Suk Bong Hong<sup>\*,†</sup>

Department of Chemical Technology, Hanbat National University, Taejon 305-719, Korea, Department of Chemical Engineering, Chungbuk National University, Chungbuk 361-763, Korea, and School of Chemical Science and Technology, Chonbuk National University, Chonju 561-757, Korea

Received: January 10, 2001; In Final Form: August 15, 2001

The <sup>1</sup>H-<sup>13</sup>C CP MAS NMR and Raman spectra of *N,N,N,N',N',N'*-hexaethylpentanediammonium (Et<sub>6</sub>-diquat-5) ions encapsulated within P1, SUZ-4, and ZSM-57 zeolites are presented. The Et<sub>6</sub>-diquat-5 molecules occluded are found to adopt distinct molecular conformations in order to fit in the pores of each zeolite host. Computer modeling studies show that encapsulation of Et<sub>6</sub>-diquat-5 in the small-pore zeolite P1 is not energetically favorable. However, a remarkable match between the conformation of guest molecule and the geometry of the host structure is observed for the medium-pore zeolites SUZ-4 and ZSM-57, revealing the existence of organic structure-directing effect. The overall results of this study suggest that conformations available to the flexible, linear organic cation like Et<sub>6</sub>-diquat-5 may differ considerably according to the type and concentration of alkali cations present in the zeolite synthesis mixture, which is a critical factor affecting the phase selectivity of the crystallization. It thus appears that the modification of conformations of flexible organic structure-directing agents by varying the type and concentration of alkali cations may be an area of considerable possibility for finding new zeolite structures.

## Introduction

The precise mechanism of the structure direction by organic additives such as amines and alkylammonium ions in the synthesis of zeolites and related materials is still poorly understood. However, it is well established that the addition of organic structure-directing agents (SDAs) to an amorphous aluminosilicate or silicate gel can affect the framework structure and/or composition of the zeolite formed.<sup>1,2</sup> In addition, they usually end up entrapped inside the void spaces of the crystallized product. Thus, detailed knowledge of the nature and extent of interactions between the occluded organic molecules and the zeolite framework is of fundamental importance in understanding the exact role of the organic SDAs during the zeolite crystallization process.

There are many examples in which the use of flexible, linear diquatery ammonium ions with the general formula R<sub>3</sub>N<sup>+</sup>(CH<sub>2</sub>)<sub>n</sub>N<sup>+</sup>R<sub>3</sub> in zeolite synthesis has enabled the discovery of novel materials.<sup>3,4</sup> Among the doubly charged ammonium cations studied thus far, the (C<sub>2</sub>H<sub>5</sub>)<sub>3</sub>N<sup>+</sup>(CH<sub>2</sub>)<sub>5</sub>N<sup>+</sup>(C<sub>2</sub>H<sub>5</sub>)<sub>3</sub> (*N,N,N,N',N',N'*-hexaethylpentanediammonium, Et<sub>6</sub>-diquat-5) ion is interesting since it is the only known SDA leading to the crystallization of ZSM-57 (MFS topology).<sup>5,6</sup> Very recently, we have attempted the synthesis of ZSM-57 using a series of (C<sub>2</sub>H<sub>5</sub>)<sub>3</sub>N<sup>+</sup>(CH<sub>2</sub>)<sub>n</sub>N<sup>+</sup>(C<sub>2</sub>H<sub>5</sub>)<sub>3</sub> with *n* = 4–6 and found that crystallization of ZSM-57 is very sensitive not only to the length of the central alkyl chain on the ammonium ion, but also to the type and the concentration of alkali cations in the synthesis

mixture.<sup>7</sup> When Et<sub>6</sub>-diquat-4 (*N,N,N,N',N',N'*-hexaethylbutanediammonium) or Et<sub>6</sub>-diquat-6 (*N,N,N,N',N',N'*-hexaethylhexanediammonium) instead of Et<sub>6</sub>-diquat-5 was added to an aluminosilicate gel with the optimized oxide composition (Na<sub>2</sub>O/SiO<sub>2</sub> = 0.30 and SiO<sub>2</sub>/Al<sub>2</sub>O<sub>3</sub> = 60) for ZSM-57 formation, for example, the obtained product is always mordenite that can also be prepared without using any organic SDA.<sup>2</sup> As Na content in the synthesis mixture was increased to Na<sub>2</sub>O/SiO<sub>2</sub> = 0.37, in addition, zeolite P1 (GIS topology) with an enhanced SiO<sub>2</sub>/Al<sub>2</sub>O<sub>3</sub> ratio of 9.8 is the phase obtained even in the presence of Et<sub>6</sub>-diquat-5. An unexpected result is that when Na<sup>+</sup> is replaced by the equivalent amount of K<sup>+</sup> under the conditions identical to those for zeolite P1, the crystallized product is SUZ-4,<sup>8</sup> a new medium-pore zeolite that is closely related to ferrierite and ZSM-57.<sup>9–11</sup> Up to now, no organic SDAs yielding SUZ-4, with the exception of the tetraethylammonium ion, have been known. While both SUZ-4 and ZSM-57 belong to the ferrierite family of zeolites, on the other hand, the 10-ring channels (4.6 × 5.2 Å) in the former zeolite are fairly smaller than the analogous channels (5.1 × 5.4 Å) in the latter zeolite. This has stimulated us to focus our interest on the host–guest interactions occurring within as-synthesized SUZ-4 and ZSM-57, as well as those within P1. Here we report the <sup>1</sup>H-<sup>13</sup>C CP MAS NMR and Raman spectra of Et<sub>6</sub>-diquat-5 encapsulated within these three zeolites, together with those of the organic in aqueous solution. The results obtained are correlated with the optimized conformations of Et<sub>6</sub>-diquat-5 molecules within zeolite hosts that are determined via computer modeling studies.

## Experimental Section

Zeolites P1, SUZ-4, and ZSM-57 were synthesized using Et<sub>6</sub>-diquat-5 as an organic SDA according to the procedures similar to those described in our previous papers.<sup>7,8</sup> The synthesis

\* Author to whom correspondence should be addressed. Phone: +82-42-821-1549. Fax: +82-42-821-1593. E-mail: sbhong@hanbat.ac.kr.

<sup>†</sup> Hanbat National University.

<sup>‡</sup> Chungbuk National University.

<sup>§</sup> Chonbuk National University.

**TABLE 1: Synthesis Conditions and Chemical Composition Data for Zeolites P1, SUZ-4, and ZSM-57**

zeolite	gel composition <sup>a</sup>	unit cell composition <sup>b</sup>	Si/Al ratio
P1	3.0Et <sub>6</sub> -diquat-5•11.0Na <sub>2</sub> O•0.5Al <sub>2</sub> O <sub>3</sub> •30SiO <sub>2</sub> •1200H <sub>2</sub> O	(Et <sub>6</sub> -diquat-5) <sub>0.3</sub> Na <sub>2.2</sub> Al <sub>2.7</sub> Si <sub>13.3</sub> O <sub>32</sub> 3.7H <sub>2</sub> O	4.9
SUZ-4	3.0Et <sub>6</sub> -diquat-5•11.0K <sub>2</sub> O•0.5Al <sub>2</sub> O <sub>3</sub> •30SiO <sub>2</sub> •1200H <sub>2</sub> O	(Et <sub>6</sub> -diquat-5) <sub>1.1</sub> K <sub>2.0</sub> Al <sub>3.9</sub> Si <sub>32.1</sub> O <sub>72</sub> 6.3H <sub>2</sub> O	8.2
ZSM-57	3.0Et <sub>6</sub> -diquat-5•9.0Na <sub>2</sub> O•0.5Al <sub>2</sub> O <sub>3</sub> •30SiO <sub>2</sub> •1200H <sub>2</sub> O	(Et <sub>6</sub> -diquat-5) <sub>0.8</sub> Na <sub>0.4</sub> Al <sub>1.4</sub> Si <sub>34.6</sub> O <sub>72</sub> 3.9H <sub>2</sub> O	25

<sup>a</sup> Crystallization was performed with stirring (100 rpm) at 160 °C for 7 days. <sup>b</sup> Determined from a combination of elemental and thermal analyses.

conditions and analyses for these three zeolites are given in Table 1. If required, as-synthesized zeolites were calcined in air at 550 °C for 6 h and refluxed twice in NH<sub>4</sub>NO<sub>3</sub> solutions for 6 h followed by calcination at 500 °C for 4 h.

The phase purity and crystallinity were determined by powder X-ray diffraction (XRD) using a Rigaku Miniflex diffractometer with Cu K $\alpha$  radiation. Chemical analysis was carried out by a combination of a Jarrell-Ash Polyscan 61E inductively coupled plasma (ICP) spectrometer, a Perkin-Elmer 5000 atomic absorption spectrophotometer, and a Carlo Erba 1106 elemental organic analyzer. Thermogravimetric analyses (TGA) were performed in air on a TA Instruments SDT 2960 thermal analyzer, where weight losses related to the combustion of organic SDA were determined from differential thermal analyses (DTA) using the same analyzer. Approximately 15 mg of sample were used at a heating rate of 10 °C min<sup>-1</sup>. The <sup>1</sup>H-<sup>13</sup>C CP MAS NMR spectra were measured on a Bruker DSX 400 spectrometer operating at <sup>13</sup>C frequency of 100.623 MHz and a spinning rate of 4.5 kHz. The spectra were obtained with an acquisition of ca. 6500 pulse transients, which was repeated with a  $\pi/2$  rad pulse length of 5.0  $\mu$ s, a contact time of 1 ms, and a recycle delay of 3 s. The <sup>13</sup>C chemical shifts are referenced to TMS. The Raman spectra in the 200–3200 cm<sup>-1</sup> region were recorded on a Bruker RFA 106/S FT-Raman spectrometer equipped with a Nd:YAG laser operating at 1064 nm. The samples were exposed to a laser power of 100–250 mW at the spectral resolution of 2 cm<sup>-1</sup>. Typically, 400–1600 scans were accumulated for obtaining the Raman spectra.

Molecular modeling studies were carried out using the Burchart-Universal force field as implemented in the Cerius<sup>2</sup> software, to determine the optimum locations and conformations of Et<sub>6</sub>-diquat-5 molecules inside the pores of zeolites studied here. The host zeolite lattice was held rigid throughout the simulation, while the Et<sub>6</sub>-diquat-5 cation occluded was mobile, to calculate the total host–guest interaction energy. No symmetry constraints were applied to the guest molecule and thus the resulting coordinate set has *P1* symmetry. The procedure was iterated until the calculated energy of interaction has reached the minimum value. The Coulombic and hydrogen-bonding interaction energies were not included in the model calculations. The unit cell parameters and atomic coordinates for P1 and ZSM-57 were taken from the original references listed in the International Zeolite Association (IZA) tabulations.<sup>12</sup> The values for SUZ-4 were adopted from a synchrotron powder XRD study reported by Lawton et al.<sup>10</sup>

## Results and Discussion

Figure 1 shows the powder XRD patterns of P1, SUZ-4, and ZSM-57 prepared here. Comparison of the patterns in Figure 1 with those in the literature<sup>9,12</sup> reveals that they are highly crystalline and no reflections other than those from the corresponding zeolites are observed. The chemical compositions of these three zeolites determined from a combination of elemental and thermal analyses are given in Table 1. There is a noticeable dissimilarity between the amount of Al and the sum of Et<sub>6</sub>-diquat-5 and alkali cations for the unit cell formula of ZSM-

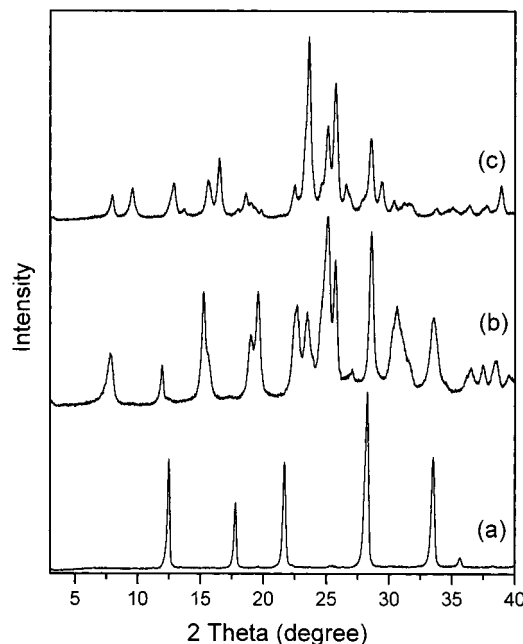


**Figure 1.** Powder X-ray diffraction patterns of as-synthesized (a) P1, (b) SUZ-4, and (c) ZSM-57.

57, unlike the case of P1 or SUZ-4. This suggests that part of the tetraalkylammonium moieties of the organic ions in ZSM-57 do not serve as charge-compensating cations but as space-filling species. The data in Table 1 also shows an enrichment of Al in each zeolite with respect to the synthesis mixture. Although this trend is more apparent to P1 and SUZ-4 than to ZSM-57, however, it should be noted that the SiO<sub>2</sub>/Al<sub>2</sub>O<sub>3</sub> ratios (9.9 and 16.5) of our P1 and SUZ-4 are significantly higher than those of previously reported isostructural materials.<sup>13,14</sup> This is not unexpected because the volume of Et<sub>6</sub>-diquat-5 is much large compared to that of the already known organic SDAs (e.g., tetramethylammonium and tetraethylammonium cations) for these two zeolites. As evidenced by XRD experiments, on the other hand, the structural integrity of all materials prepared here remains intact during the initial calcinations at 550 °C to remove the occluded Et<sub>6</sub>-diquat-5 molecules. In the case of SUZ-4 and ZSM-57, in addition, no detectable loss of crystallinity is caused by the successive NH<sub>4</sub><sup>+</sup> ion exchange and calcination steps to prepare the acid form. After NH<sub>4</sub><sup>+</sup> ion exchange, however, zeolite P1 was found to begin losing crystallinity at 400 °C, reflecting a poor stability of its acid form, despite the enhanced SiO<sub>2</sub>/Al<sub>2</sub>O<sub>3</sub> ratio.

Figure 2 shows the TGA/DTA curves for as-synthesized P1, SUZ-4, and ZSM-57. Zeolite P1 gives two stages of weight loss: 25–200 and 450–550 °C. The first loss is endothermic and can be assigned to the desorption of water. The second loss is accompanied by a small exotherm around 480 °C, revealing that it must be from the thermal decomposition of Et<sub>6</sub>-diquat-5. This result is somehow surprising, since two 8-ring channels (3.1 × 4.5 Å and 2.8 × 4.8 Å) in P1 and even its channel intersections are not large enough to accommodate the bulky Et<sub>6</sub>-diquat-5 ion. However, it is well-known that P1 has

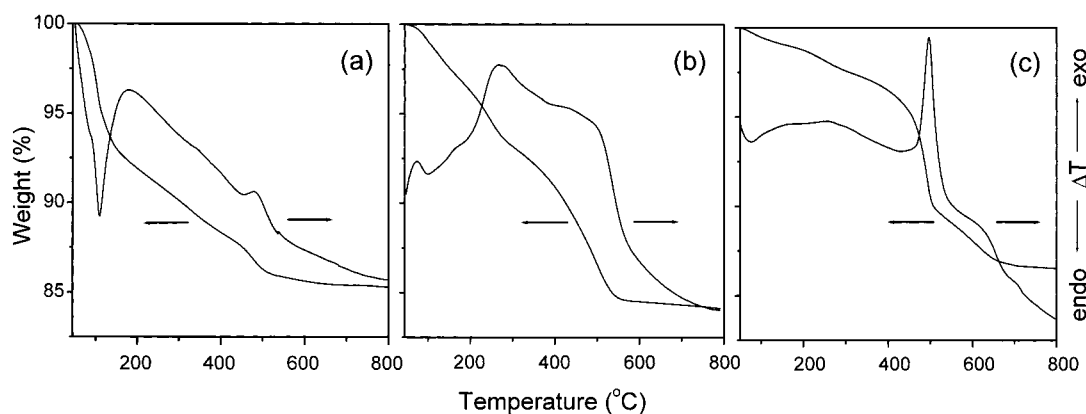


Figure 2. TGA/DTA curves for as-synthesized (a) P1, (b) SUZ-4, and (c) ZSM-57.

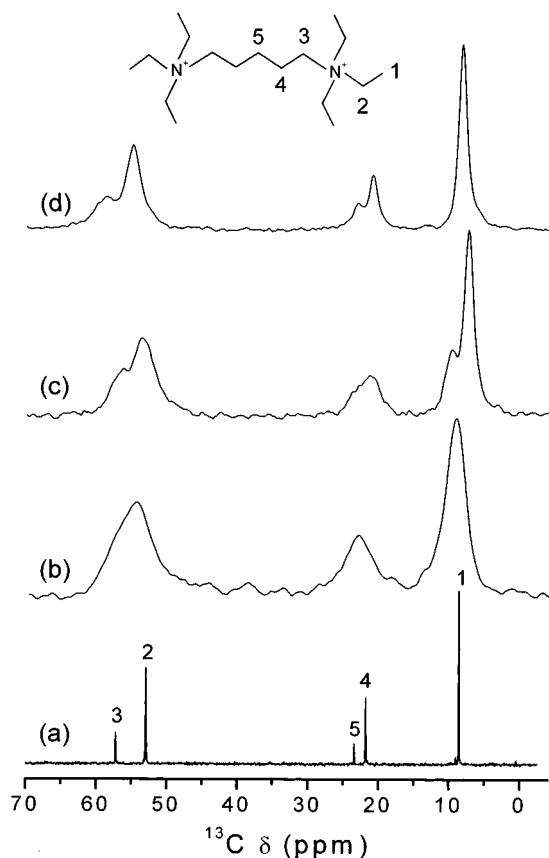


Figure 3.  $^{13}\text{C}$  NMR spectra of organic SDA,  $\text{Et}_6\text{-diquat-5}$ :  $^{13}\text{C}$  NMR of a  $\text{CDCl}_3$  solution of the (a) bromide form of  $\text{Et}_6\text{-diquat-5}$  and  $^1\text{H}$ - $^{13}\text{C}$  CP MAS NMR of as-synthesized (b) P1, (c) SUZ-4, and (d) ZSM-57 with  $\text{Et}_6\text{-diquat-5}$  occluded in their pores, showing the assignment of each resonance.

considerable framework flexibility.<sup>15</sup> We believe that this may be responsible for the encapsulation of  $\text{Et}_6\text{-diquat-5}$  in this small-pore zeolite. Like P1, SUZ-4 shows one exothermic weight loss at 250–550 °C assigned to the combustion of  $\text{Et}_6\text{-diquat-5}$ . As seen in Figure 2, however, the decomposition pattern of the organic in ZSM-57 is characterized by two weight losses at 250–500 and 500–700 °C that have distinct exothermic peaks in the DTA. This results is consistent with that reported by Ernst and Weitkamp.<sup>16</sup> The TGA/DTA curves (not shown) of the proton form of ZSM-57 gave no detectable exothermic peaks in the temperature region higher than 500 °C, suggesting that the high-temperature weight loss is not due to dehydroxylation of Brönsted acid sites in ZSM-57. It thus appears that the high-

TABLE 2:  $^1\text{H}$ - $^{13}\text{C}$  MAS NMR Chemical Shift Data for  $\text{Et}_6\text{-diquat-5}$

chemical shift (fwhm <sup>a</sup> ), ppm from TMS			
$\text{CDCl}_3$	P1	SUZ-4	ZSM-57
8.2	8.8 (350)	6.6 (380)	8.4 (140)
21.6	22.8 (480)	9.1 (250)	21.2 (170)
23.3		20.6 (360)	23.3 (210)
53.5	54.4 (660)	22.7 (430)	55.3 (280)
57.7		53.1 (550)	59.0 (430)
		55.6 (530)	

<sup>a</sup> Full width at half-maximum of the  $^1\text{H}$ - $^{13}\text{C}$  MAS NMR band in Hz.

temperature DTA peak is due to oxidation of products arising from incomplete combustion of  $\text{Et}_6\text{-diquat-5}$  below 500 °C.

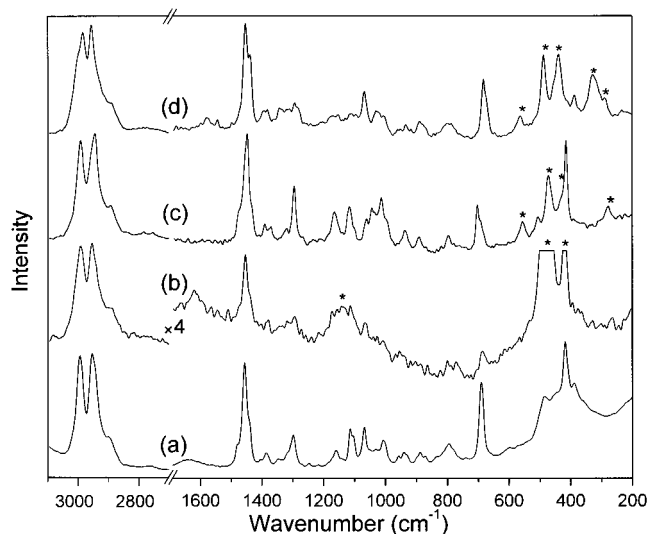
Figure 3 shows the  $^1\text{H}$ - $^{13}\text{C}$  CP MAS NMR spectra of as-synthesized P1, SUZ-4, and ZSM-57 together with the liquid  $^{13}\text{C}$  NMR spectrum of a  $\text{CDCl}_3$  solution of the  $\text{Et}_6\text{-diquat-5}$  bromide salt. The assignments of the observed resonances are also indicated in Figure 3, and their chemical shifts and line widths are given in Table 2. These data clearly show that  $\text{Et}_6\text{-diquat-5}$  not only remains intact upon its occlusion into the pores of zeolites prepared here, but also it experiences the chemical environment that is distinctly different in each of these three materials. On the basis of the  $^1\text{H}$ - $^{13}\text{C}$  CP MAS NMR results, therefore, it is clear that the extent of changes in the conformation of  $\text{Et}_6\text{-diquat-5}$  is significantly different in each of these three zeolites. When the cation is located inside the pores of P1, for example, the resonance of the methyl carbon is observed at 8.8 ppm and thus is shifted downfield relative to the corresponding carbon resonance of free  $\text{Et}_6\text{-diquat-5}$  bromide. Despite the fact that two different types of methylene carbons adjacent to the nitrogen exist in  $\text{Et}_6\text{-diquat-5}$ , in particular, the  $^1\text{H}$ - $^{13}\text{C}$  CP MAS NMR spectrum of P1 shows only one broad resonance at 54.4 ppm where two resonances should be otherwise observed. A similar trend is also observed for the case of the second and third methylene carbons in the central pentyl chain, due to the appearance of a single resonance at 22.8 ppm. These results reveal that the bulky  $\text{Et}_6\text{-diquat-5}$  molecule is so tightly fit within the 8-ring pores of P1 as to make it very difficult to distinguish the two different methylene carbons bonded to the nitrogen or those in the pentyl chain, leading to the dramatic reduction in the mobility of the occluded organic molecule. Here we note that there are two additional resonances around 37 and 19 ppm in the  $^{13}\text{C}$  MAS NMR spectrum of P1, which are assignable to methylene and methyl carbons of triethylamine ( $\text{Et}_3\text{N}$ ), respectively.<sup>17</sup> This suggests that the decomposition of  $\text{Et}_6\text{-diquat-5}$  leading to the formation of  $\text{Et}_3\text{N}$  during the crystallization of P1 is possible, due to the



highly basic nature (pH  $\sim$ 13.6) of the synthesis mixture. However, the fact that the two resonances appearing around 37 and 19 ppm are much weaker than the resonances from Et<sub>6</sub>-diquat-5 clearly shows that most of the organic SDAs used for P1 synthesis have not decomposed under the crystallization conditions but remained intact.

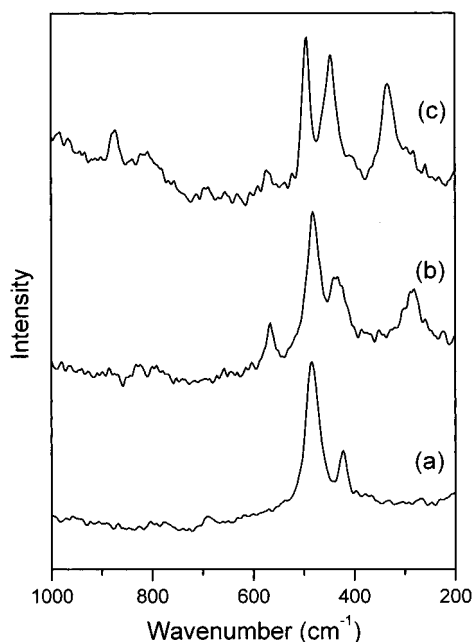
An interesting observation obtained from Figure 3 is that encapsulation of Et<sub>6</sub>-diquat-5 within the pores of SUZ-4 gives rise to the splitting of the methyl carbon resonance into two peaks at 6.6 and 9.1 ppm. Unlike those of the organic molecule in P1, in addition, all the methylene carbon resonances of Et<sub>6</sub>-diquat-5 occluded in SUZ-4 can be resolved, but are shifted slightly upfield relative to those of free Et<sub>6</sub>-diquat-5. There are numerous examples where <sup>13</sup>C MAS NMR spectroscopy has been extensively employed to elucidate the location and conformation of organic SDAs occluded into the zeolites during the crystallization process.<sup>18</sup> Especially germane to this is the case of tetrapropylammonium (TPA) ions in ZSM-5. Splitting of the methyl carbon resonance of TPA has been repeatedly observed and related to differences in the chemical environment of the two types of 10-ring channels in ZSM-5.<sup>18–20</sup> A subsequent Rietveld refinement of the powder X-ray diffraction data<sup>21</sup> confirmed that the TPA cation is located in the channel intersection with two of the propyl chains extending into the linear channel and two into the sinusoidal channel. Considering that SUZ-4 contains a two-dimensional pore system consisting of two intersecting 10- and 8-ring channels, therefore, splitting of the methyl carbon resonance of Et<sub>6</sub>-diquat-5 occluded in SUZ-4 could be understood in a manner similar to that from TPA in ZSM-5. If such is the case, four of the ethyl groups of Et<sub>6</sub>-diquat-5 in SUZ-4 may extend into the 8-ring channel and two into the 10-ring channel. This speculation was based on the fact that the relative intensity ratio of the two methyl carbon resonances appearing at 6.6 and 9.1 ppm in the spectrum of SUZ-4 is approximately 2:1. Regardless of the exact assignment of the <sup>1</sup>H-<sup>13</sup>C CP MAS NMR spectrum for SUZ-4, however, it is clear that the observed splitting of the methyl resonance is characteristic of the conformation adopted by Et<sub>6</sub>-diquat-5 in the SUZ-4 channel intersection, which may originate from differences in the van der Waals interactions between the methyl groups in 10-ring channels and those in 8-ring channels. In contrast to the organic molecule in SUZ-4, on the other hand, the Et<sub>6</sub>-diquat-5 occluded in ZSM-57 gives only one methyl carbon resonance at 8.4 ppm that is essentially unchanged relative to that of free Et<sub>6</sub>-diquat-5. While the chemical shifts of the resonances of the second and third methylene carbons in the pentyl chain of the occluded diammonium ion are similar to those observed for free Et<sub>6</sub>-diquat-5, in addition, the resonances at 53.5 and 57.7 ppm, due to the inequivalence of the two methylene carbons bonded to the nitrogen, are shifted downfield relative to those of free Et<sub>6</sub>-diquat-5. The absence of splitting of the methyl carbon resonance indicates that unlike those of the organic in SUZ-4, the methyl groups of Et<sub>6</sub>-diquat-5 in ZSM-57 do not experience severe geometric constraints and van der Waals interactions with the zeolite framework, which may be due to the fairly large size of its channel intersections. This can be further supported by the fact that the full widths at half-maximum (fwhm's) of all carbon resonances observed for ZSM-57 are considerably smaller than those of the corresponding carbons from SUZ-4 (see Table 2).

Figure 4 shows the Raman spectra of as-synthesized P1, SUZ-4, and ZSM-57 in the 200–3100 cm<sup>−1</sup> region. The Raman spectrum of Et<sub>6</sub>-diquat-5 in aqueous solution is also compared in Figure 4. In agreement with the <sup>1</sup>H-<sup>13</sup>C CP MAS NMR data



**Figure 4.** Raman spectra in the 200–3100 cm<sup>−1</sup> region of (a) 0.5 M aqueous solution of Et<sub>6</sub>-diquat-5 bromide and as-synthesized (b) P1, (c) SUZ-4, and (d) ZSM-57. Structural Raman bands of each zeolite are marked by asterisks.

given above, Raman spectroscopy reveals that Et<sub>6</sub>-diquat-5 remains intact upon its occlusion into the pores of SUZ-4 and ZSM-57. The same result can be observed for P1, although it exhibits weak Raman features of Et<sub>6</sub>-diquat-5 due to its low concentration of the organic occluded (Table 1). It is clear from Figure 4 that many spectral changes take place, especially in the case of ZSM-57, as the organic cation is trapped inside the zeolite pores. To date, there are neither published vibrational spectra of free Et<sub>6</sub>-diquat-5 nor normal-coordinate calculations on this organic molecule. Thus, the unequivocal assignment and interpretation of most of the changes found in Figure 4 cannot be made at this time. However, some of them provide clear evidence that host–guest interactions occurring within zeolites prepared here are significantly different from one another. Based on comparison with various tetralkylammonium salts,<sup>22</sup> for example, the band appearing at 693 cm<sup>−1</sup> in the Raman spectrum of Et<sub>6</sub>-diquat-5 in aqueous solution can be tentatively assigned to the C–N stretching mode. As seen in Figure 4, however, SUZ-4 exhibits a band at 709 cm<sup>−1</sup> with a shoulder around 697 cm<sup>−1</sup>. The splitting and blue-shift of the C–N stretching mode with respect to the corresponding vibration mode of free Et<sub>6</sub>-diquat-5 suggest that the mirror symmetry of the organic molecule is removed upon its occlusion into the pores of SUZ-4 and thus the two halves of the occluded molecule are no longer equal to each other. By contrast, the Raman spectrum in the C–N stretching region of ZSM-57 is characterized by one rather asymmetric band centered at 687 cm<sup>−1</sup> that is considerably red-shifted compared to that observed for SUZ-4. This can be rationalized by considering that the 10-ring channels (5.1 × 5.4 Å) in ZSM-57 are fairly larger than those (4.6 × 5.2 Å) in SUZ-4. It has been repeatedly shown that the band positions of specific skeletal Raman vibration modes of the guest molecule in zeolites are sensitive to the size of the zeolite pores where the molecule is trapped.<sup>23–25</sup> Figure 4 also shows that a strong band appearing at 419 cm<sup>−1</sup> in the Raman spectra of free Et<sub>6</sub>-diquat-5 and SUZ-4, assignable to the C–N bending mode, is completely missing in the Raman spectrum of as-synthesized ZSM-57. In addition to perturbations on the C–N bond, the Raman signature of occluded Et<sub>6</sub>-diquat-5 includes notable differences in the band position and intensity of the CH<sub>2</sub> wagging mode at 1300–1350 cm<sup>−1</sup>, the CH<sub>3</sub> deformation mode at 1440–1465 cm<sup>−1</sup>, and the CH stretching modes at 2850–



**Figure 5.** Raman spectra in the structural region of (a) P1, (b) SUZ-4, and (c) ZSM-57 calcined at 550 °C for 6 h.

3050  $\text{cm}^{-1}$ . Therefore, it is clear that the  $\text{Et}_6$ -diquat-5 molecules in aqueous solutions, SUZ-4 and ZSM-57 adopt conformations distinctly different from one another, which is mainly due to the difference in geometrical restrictions imposed by the particular framework topology of each zeolite.

According to the Raman data of zeolite frameworks published thus far, on the other hand, the most prominent band is always found in the 300–550  $\text{cm}^{-1}$  region and is assigned to the motion of the framework oxygen atom in the plane perpendicular to the T–O–T band. Dutta et al.<sup>26,27</sup> reported that zeolites with even-numbered rings such as 4-, 6-, 8-, 10-, and 12-rings exhibit the T–O–T bending vibration band in the 480–520  $\text{cm}^{-1}$  region, while the presence of 5-rings in the framework as in ZSM-5, mordenite, and ZSM-48 leads to a lowering of its position to the 390–460  $\text{cm}^{-1}$  region. Based on these findings, they suggested that the position of the T–O–T bending mode could be empirically correlated with the ring systems present in the zeolite frameworks. To evaluate whether this empirical correlation is useful for the identification of specific structural units in zeolites, we have recorded the Raman spectra of calcined P1, SUZ-4, and ZSM-57. The spectra in the structural region of these three materials are compared in Figure 5. These data reveal that calcined P1, SUZ-4, and ZSM-57 exhibit the most prominent band at 483, 481, and 493  $\text{cm}^{-1}$ , respectively. Recall that the P1 structure is composed of 4- and 8-rings, while the framework topologies of both SUZ-4 and ZSM-57 are characterized by combinations of 4-, 5-, 6-, 8-, and 10-rings.<sup>10,28</sup> Despite the presence of 5-rings in SUZ-4 and ZSM-57, therefore, no significant differences in the position of the most prominent band from all zeolites studied here are observed. This led us to conclude that no empirical correlation exists between the structural units present in zeolites and the Raman band position of the T–O–T bending mode. In fact, theoretical studies on the vibrational spectra of zeolites have shown that the characteristics of isolated cluster (ring) models disappear when the cluster is embedded into a periodic zeolite structure.<sup>29,30</sup>

To gain additional information regarding the host–guest interactions occurring within zeolites prepared here, we have attempted to optimize the locations and conformations of the occluded  $\text{Et}_6$ -diquat-5 molecules via energy minimization

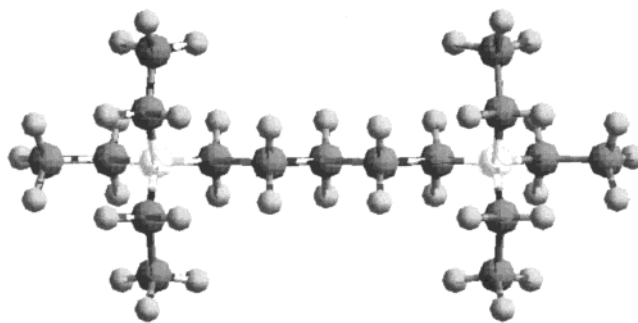


**Figure 6.** Model of the lowest-energy conformation for free  $\text{Et}_6$ -diquat-5. Carbon, nitrogen, and hydrogen atoms are shown as large gray, white, and small gray balls, respectively.

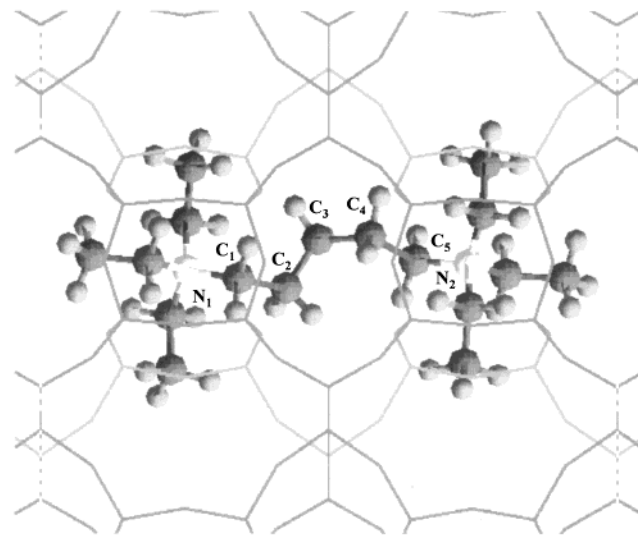


**Figure 7.** Optimized conformation for a single  $\text{Et}_6$ -diquat-5 molecule inside 10-ring channels running along the [001] direction of SUZ-4. The framework, depicted in a stick model, is viewed in the projection down the [010] direction where 8-ring channels are running.

calculations. Since the crystal structure of the pure  $\text{Et}_6$ -diquat-5 bromide remains unknown, the initial focus of our modeling studies was placed on the lowest-energy conformation for the free organic molecule. The best model for free  $\text{Et}_6$ -diquat-5 that does not violate any geometrical constraints is shown in Figure 6. This model indicates that the ethyl groups adopt an all-trans configuration, if only the rotation with respect to the C–N bond involving the methylene carbons of ethyl groups is considered. Apparently, any deviation from the all-trans form of the ethyl groups can introduce considerable nonbonded interactions of the hydrogen atoms, due to branching of hydrocarbon chains at the nitrogen atom. The same result can also be observed for the central pentyl chain of the free organic molecule. Using a set of coordinates for free  $\text{Et}_6$ -diquat-5, we inserted the organic molecule into the P1, SUZ-4, and ZSM-57 structures, respectively, at a random orientation and then performed energy minimization calculations that allowed for atomic displacements of the  $\text{Et}_6$ -diquat-5 molecule with the lowest energy.

Figure 7 shows the lowest-energy conformation for  $\text{Et}_6$ -diquat-5 inside the SUZ-4 framework containing two channel intersections per unit cell and a 10-ring channel. Computer simulation predicts one  $\text{Et}_6$ -diquat-5 molecule per unit cell, which is in reasonable agreement with the value determined from TGA/DTA (see Table 1). A calculated interaction energy of  $-85 \text{ kJ mol}^{-1}$  per  $\text{Et}_6$ -diquat-5 molecule was obtained, and the van der Waals interaction was found to be the most important contributor toward favorable host–guest interactions. Figure 7

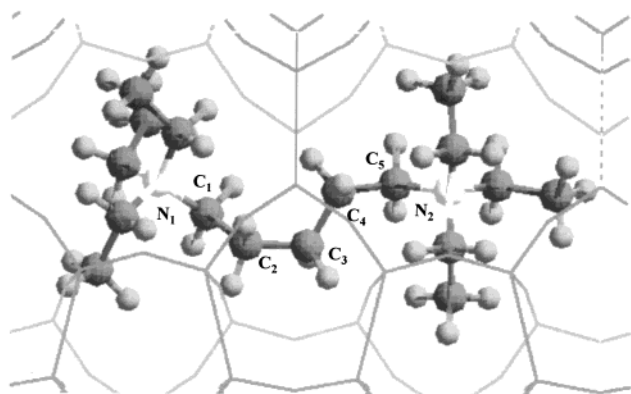


**Figure 8.** Optimized conformation for one Et<sub>6</sub>-diquat-5 molecule inside 10-ring channels running along the [100] direction of ZSM-57. The framework is viewed in the projection down the [010] direction where 8-ring channels are running.

clearly shows that four of the ethyl groups of Et<sub>6</sub>-diquat-5 are positioned within the 8-ring channel, while two are positioned within the 10-ring channel. Thus, a close match between the geometry of the organic molecule and that of the peculiar pore structure of SUZ-4 with intersecting 10- and 8-ring channels is found. Notice that such a match is in excellent agreement with that deduced from <sup>1</sup>H-<sup>13</sup>C CP MAS NMR spectroscopy. Figure 7 also reveals that although all the ethyl groups of Et<sub>6</sub>-diquat-5 in SUZ-4, like those in free Et<sub>6</sub>-diquat-5, adopt an all-trans configuration, there are gauche interactions with respect to the C<sub>1</sub>–C<sub>2</sub> and C<sub>3</sub>–C<sub>4</sub> bonds in the central pentyl chain. Since the C<sub>2</sub>–C<sub>3</sub> and C<sub>4</sub>–C<sub>5</sub> bonds in the central chain adopt a trans configuration, however, no severe geometric constraints imposed on the guest molecule upon encapsulation into the two-dimensional pore system of SUZ-4 are caused. These results again confirm that Et<sub>6</sub>-diquat-5 in SUZ-4 adopts a conformation distinctly different from that of the free organic molecule in order to fit in the channel intersection.

A similar conclusion can be drawn from the case of Et<sub>6</sub>-diquat-5 occluded in ZSM-57. One Et<sub>6</sub>-diquat-5 molecule is accommodated in the unit cell, as seen in Figure 8, with a half per channel intersection. The interaction energy for Et<sub>6</sub>-diquat-5 in ZSM-57 was calculated to be –180 kJ mol<sup>–1</sup> per molecule, which is considerably low compared to the value obtained from SUZ-4. This is not unexpected because all the ethyl groups of Et<sub>6</sub>-diquat-5 in ZSM-57 do not extend into the 8-ring channel but lie in the channel intersection, giving them weaker geometric constraints and van der Waals interactions with the zeolite framework. An important observation is that the C<sub>2</sub>–C<sub>3</sub> and C<sub>4</sub>–C<sub>5</sub> bonds in the central pentyl chain adopt a gauche configuration, while the C<sub>1</sub>–C<sub>2</sub> and C<sub>3</sub>–C<sub>4</sub> bonds in the corresponding chain do a trans configuration. From analysis of the rotations about the four C–C bonds within the central pentyl chain, in addition, we note that the calculated rotation angles of individual C–C bonds of the Et<sub>6</sub>-diquat-5 molecule occluded in ZSM-57 are significantly different from those of the corresponding C–C bonds of the guest molecule in SUZ-4. As a result, none of the three ethyl groups around the C<sub>1</sub>–N<sub>1</sub> bond are in the same direction as that of 8-ring channels, as seen in Figure 8, unlike the case of the guest molecule in SUZ-4. Therefore, it appears that the geometric correspondence between the Et<sub>6</sub>-diquat-5 molecule and the zeolite structure is less close in ZSM-57 than in SUZ-4, although the structure-directing role of Et<sub>6</sub>-diquat-5 in the crystallization of both zeolites is evident. This can readily be understood by the fact that the 10-ring channels in ZSM-57 are fairly large compared to those in SUZ-4.

Molecular modeling studies showing that the match between the shape of Et<sub>6</sub>-diquat-5 at its optimized location and that of the two-dimensional channel system of ZSM-57 is significantly different from that of this study have reported by Stevens et al.<sup>31</sup> In fact, their optimized conformation was found to be quite similar to that of the organic molecule in SUZ-4 obtained here. The discrepancy with our simulation data on Et<sub>6</sub>-diquat-5 in ZSM-57 appears to be due to differences in the force field and the parameters employed in the respective simulations. In contrast to those obtained from the two systems investigated above, on the other hand, molecular modeling studies on Et<sub>6</sub>-diquat-5 in P1 with two intersecting 8-ring channels gave a calculated stabilization energy of about 1100 kJ mol<sup>–1</sup> per molecule. This indicates that encapsulation of the Et<sub>6</sub>-diquat-5 molecules in the P1 pores is not energetically favorable. As described earlier, however, a combination of TGA/DTA, <sup>1</sup>H-<sup>13</sup>C CP MAS NMR, and Raman measurements clearly shows the occlusion of Et<sub>6</sub>-diquat-5 into the P1 pores. This again confirms the remarkable framework flexibility of P1, since the P1 lattice has been assumed to be rigid throughout the whole modeling process. It thus appears that during the synthesis of P1, Et<sub>6</sub>-diquat-5 is not acting as an SDA but rather as a space-filling species.

It is well-known that some zeolites can be synthesized using a wide range of organic SDAs. It is also true that some organic SDAs can produce more than one zeolite structure, depending on the oxide composition of synthesis mixtures and/or the crystallization conditions employed.<sup>13</sup> A good example of the latter case is the tetraethylammonium (TEA) cation that can direct the synthesis of zeolites beta, ZSM-5, ZSM-12, SUZ-4, etc. Due to notable differences in the pore structure of these zeolites, the TEA cations occluded should be required to adopt distinct conformations that are closely related to the structural aspects of each zeolite host, as evidenced by the theoretical and neutron scattering studies of Brand et al.<sup>32</sup> On the other hand, the number of conformations available to the linear diquatary Et<sub>6</sub>-diquat-5 cation must be much larger than that for the relatively small, symmetric TEA cation. This is not unexpected because Et<sub>6</sub>-diquat-5 is much more flexible than TEA. We have recently shown that the structure-directing effect exerted by Et<sub>6</sub>-diquat-5 itself is not strong enough to govern the synthesis of SUZ-4 and ZSM-57, because the phase selectivity of the crystallization is sensitive to the oxide composition of the synthesis mixture, especially to the type and concentration of alkali cations used.<sup>7,8</sup> This implies that the choice of alkali cations with a certain level of concentration is the major factor determining the conformation of Et<sub>6</sub>-diquat-5 that should affect the nucleation process and ultimately the crystal structure formed. It has long been recognized that the alkali cations may influence the structure of aluminosilicate or silicate species in the zeolite synthesis mixture, as well as their distribution.<sup>33–35</sup> For example, Na<sup>+</sup> serves as a structure-making agent to interact strongly with surrounding inorganic components during the crystallization process of zeolites. However, the larger K<sup>+</sup> acts as a structure-breaking agent that is not strong enough to form organized silicate structures. Thus, we believe that the flexible, linear Et<sub>6</sub>-diquat-5 molecule may happen to be surrounded in a single or a few closely related conformations, depending on the type and concentration of alkali cations in the synthesis mixture. This may make it possible to considerably differ the conformation of the organic molecule in the Na<sup>+</sup>-containing synthesis mixture from that in the K<sup>+</sup>-containing synthesis mixture. Additionally, we believe that if the energy differences between conformations and the barriers to interconversion are not so



large, the higher energy conformations could readily be accessible under the zeolite crystallization conditions. These arguments in total led us to conclude that the modification of molecular conformations of flexible organic SDAs such as Et<sub>6</sub>-diquat-5 by varying the type and concentration of alkali cations could be an area of considerable possibility for finding new zeolite structures. We are investigating the Et<sub>6</sub>-diquat-5-mediated synthesis of zeolites in crystallization conditions other than those employed for the synthesis of SUZ-4 or ZSM-57 in order to find novel materials, and evidence to support the conclusion given above will be described in our future paper.

## Conclusions

The host–guest interactions in P1, SUZ-4, and ZSM-57 zeolites containing Et<sub>6</sub>-diquat-5 as a guest molecule are investigated by thermal analyses, <sup>1</sup>H-<sup>13</sup>C CP MAS NMR and Raman spectroscopies, and molecular modeling studies. It is found that the conformations of Et<sub>6</sub>-diquat-5 molecules encapsulated within the pores of these three zeolites are distinctly different from one another. The overall results obtained here suggest that the molecular conformations of flexible, linear organic cation like Et<sub>6</sub>-diquat-5 can be distinctly modified by varying the type and concentration of alkali cations in the zeolite synthesis mixture, which should affect the phase selectivity of the crystallization. This led us to believe that the combined use of a flexible organic cation and an alkaline cation as SDAs could lead to the discovery of novel zeolite structures.

**Acknowledgment.** We are thankful for the financial support of the Korea Research Foundation (KRF-1999-E00346) and the Korea Science and Engineering Foundation through the Advanced Materials Research Center for a Better Environment at Hanbat National University. We also thank the reviewers for the valuable comments and discussions.

## References and Notes

- (1) Lok, B. M.; Cannan, T. R.; Messina, C. A. *Zeolites* **1983**, 3, 282.
- (2) Lobo, R. L.; Zones, S. I.; Davis, M. E. *J. Inclusion Phenom. Mol. Recognit. Chem.* **1996**, 21, 47.
- (3) Szostak, R. *Handbook of Molecular Sieves*; Van Nostrand Reinhold: New York, 1992.
- (4) Moini, A.; Schmitt, K. D.; Valyocik, E. W.; Polomski, R. F. *Zeolites* **1994**, 14, 504.
- (5) Valyocik, E. W.; Page, N. M. Eur. Pat. Appl. 0 174 121, 1986.
- (6) Schlenker, J. L.; Higgins, J. B.; Valyocik, E. W. *Zeolites* **1990**, 10, 293.
- (7) Lee, S.-H.; Lee, D.-K.; Shin, C.-H.; Paik, W. C.; Lee, W. M.; Hong, S. B. *J. Catal.* **2000**, 196, 158.
- (8) Paik, W. C.; Shin, C.-H.; Hong, S. B. *Chem. Commun.* **2000**, 1609.
- (9) Barri, S. I. Eur. Pat. Appl. 0 353 915, 1990.
- (10) Lawton, S. L.; Bennett, J. M.; Schlenker, J. L.; Rubin, M. K. *J. Chem. Soc., Chem. Commun.* **1993**, 894.
- (11) Asensi, M. A.; Cambor, M. A.; Martinez, A. *Microporous Mesoporous Mater.* **1999**, 28, 427.
- (12) Treacy, M. M. J.; Higgins, J. B.; von Ballmoos, R. *Collection of Simulated XRD Patterns for Zeolites*; Elsevier: London, 1996.
- (13) Szostak, R. *Handbook of Molecular Sieves*; Van Nostrand Reinhold: New York, 1987.
- (14) Baerlocher, Ch.; Meier, W. M. *J. Helv. Chim. Acta* **1970**, 53, 1285.
- (15) Breck, D. W. *Zeolite Molecular Sieves*; Wiley: Chichester, 1974; p 73.
- (16) Ernst, S.; Weitkamp, J. *Stud. Surf. Sci. Catal.* **1991**, 65, 645.
- (17) Breitmaier, Voelter, W. *<sup>13</sup>C NMR Spectroscopy*, 2nd Ed.; Verlag Chemie: Weinheim, 1978; p 178.
- (18) Engelhardt, G.; Michel, D. *High-Resolution Solid-State NMR of Silicates and Zeolites*; Wiley: Chichester, 1987.
- (19) Boxhoorn, G.; van Santen, R. A.; van Erp, W. A.; Huis, G. R.; Clague, D. J. *Chem. Soc., Chem. Commun.* **1982**, 264.
- (20) Nagy, J. B.; Gabelica, Z.; Derouane, E. G. *Zeolites* **1983**, 3, 43.
- (21) Baerlocher, Ch. *Proceedings of the Sixth Zeolite International Conference*; Olson, D., Bisio, A., Eds.; Butterworth: Guildford, England, 1984; p 823.
- (22) Lin-Vien, D.; Colthup, N. B.; Fateley, W. G.; Grasselli, J. G. *Handbook of Infrared and Raman Characteristic Frequencies of Organic Molecules*; Academic: San Diego, 1991.
- (23) Dutta, P. K.; Del Barco, B.; Shieh, D. C. *Chem. Phys. Lett.* **1986**, 127, 200.
- (24) Hong, S. B. *Microporous Mater.* **1995**, 4, 309.
- (25) Hong, S. B.; Cambor, M. A.; Davis, M. E. *J. Am. Chem. Soc.* **1997**, 119, 761.
- (26) Dutta, P. K.; Shieh, D. C.; Puri, M. *Zeolites* **1988**, 8, 306.
- (27) Dutta, P. K.; Rao, K. M.; Park, J. Y. *J. Phys. Chem.* **1991**, 95, 6654.
- (28) Meier, W. M.; Olson, D. H.; Baerlocher, Ch. *Atlas of Zeolite Structure Types*, 4th ed.; Elsevier: London, 1996.
- (29) van Santen, R. A.; Vogel, *Adv. Solid State Chem. Soc.* **1989**, 1, 151.
- (30) Buckley, R. G.; Deckman, H. W.; Newsam, J. M.; McHenry, J. A.; Persans, P. D.; Witzke, H. *Mater. Res. Soc. Symp. Proc.* **1988**, 111, 141.
- (31) Stevens, A. P.; Gorman, A. M.; Freeman, C. M.; Cox, P. A. *J. Chem. Soc., Faraday Trans.* **1996**, 92, 2065.
- (32) Brand, H. V.; Curtiss, L. A.; Iton, L. E.; Trouw, F. R.; Brun, T. O. *J. Phys. Chem.* **1994**, 98, 1293.
- (33) Depasse, J.; Watillon, A. *J. Coll. Interface Sci.* **1970**, 33, 431.
- (34) Iler, R. K. *The Chemistry of Silica*; Wiley: New York, 1979.
- (35) Feijen, E. J. P.; Martens, J. A.; Jacobs, P. A. *Stud. Surf. Sci. Catal.* **1994**, 84, 3.